Acta Pharmaceutica Sinica B 2019;9(4):782–793

Chinese Pharmaceutical Association
Institute of Materia Medica, Chinese Academy of Medical Sciences

Acta Pharmaceutica Sinica B

www.elsevier.com/locate/apsb
www.sciencedirect.com

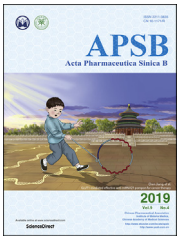

ORIGINAL ARTICLE

Chrysophanol protects against doxorubicin-induced cardiotoxicity by suppressing cellular PARylation

Jing Lu[a,†], Jingyan Li[a,†], Yuehuai Hu[a], Zhen Guo[a], Duanping Sun[b], Panxia Wang[a], Kaiteng Guo[a], Dayue Darrel Duan[c], Si Gao[d], Jianmin Jiang[a], Junjian Wang[a,*], Peiqing Liu[a,*]

[a]*School of Pharmaceutical Sciences, Sun Yat-sen University, Guangzhou 510006, China*
[b]*Guangzhou Key Laboratory of Construction and Application of New Drug Screening Model Systems, Guangdong Pharmaceutical University, Guangzhou 510006, China*
[c]*Laboratory of Cardiovascular Phenomics, Department of Pharmacology, University of Nevada Reno School of Medicine, Reno, NV 89557, USA*
[d]*School of Medicine, Guangxi University of Science and Technology, Liuzhou 545005, China*

Received 11 August 2018; revised 26 September 2018; accepted 9 October 2018

KEY WORDS

Chrysophanol;
Doxorubicin;
PARylation;
Cardiotoxicity;
Apoptosis;
Mitochondria

Abstract The clinical application of doxorubicin (DOX) in cancer chemotherapy is limited by its life-threatening cardiotoxic effects. Chrysophanol (CHR), an anthraquinone compound isolated from the rhizome of *Rheum palmatum* L., is considered to play a broad role in a variety of biological processes. However, the effects of CHR's cardioprotection in DOX-induced cardiomyopathy is poorly understood. In this study, we found that the cardiac apoptosis, mitochondrial injury and cellular PARylation levels were significantly increased in H9C2 cells treated by Dox, while these effects were suppressed by CHR. Similar results were observed when PARP1 activity was suppressed by its inhibitors 3-aminobenzamide (3AB) and ABT888. Ectopic expression of PARP1 effectively blocked this CHR's cardioprotection against DOX-induced cardiomyocyte injury in H9C2 cells. Furthermore, pre-administration with both CHR and

Abbreviations: ADR, adriamycin; ANOVA, one-way analysis of variance; CHR, chrysophanol; CMC-Na, sodium carboxymethyl; CO, cardiac output; Cyt *c*, Cytochrome *c*; DOX, doxorubicin; EF, ejection fraction; FBS, fetal bovine serum; FS, fractional shortening; HE, hematoxylin-eosin; HR, heart rate; IVSd, end-diastolic interventricular septum; IVSs, end-systolic interventricular septum; LV, end-systolic volume; LVEDV, LV end-diastolic volume; LVIDd, LV end-diastolic internal diameter; LVIDs, LV end-systolic internal diameter; LVPWd, LV end-diastolic posterior wall thickness; LVPWs, LV end-systolic posterior wall thickness; NS, normal saline; PARP1, poly(ADP-ribose) polymerase 1; PARylation, poly(ADP-ribosyl)ation; PAR, polymers of ADP-ribose; PARylated, poly(ADP-ribosyl)ated; PBS, phosphate-buffered saline; RCR, respiratory control ratio; Rh123, rhodamine 123; ROS, reactive oxygen species; SD, Sprague–Dawley; TUNEL, TdT-mediated dUTP nick end labeling; VDAC1, voltage dependent anion channel 1; 3AB, 3-aminobenzamide

*Corresponding authors. Tel.: +86 20 39943116; fax: +86 20 39943026.
E-mail address: wangjj87@mail.sysu.edu.cn (Junjian Wang), liupq@mail.sysu.edu.cn (Peiqing Liu).
†These authors made equal contributions to this paper.

Peer review under responsibility of Institute of Materia Medica, Chinese Academy of Medical Sciences and Chinese Pharmaceutical Association.

https://doi.org/10.1016/j.apsb.2018.10.008

3AB relieved DOX-induced cardiac apoptosis, mitochondrial impairment and heart dysfunction in Sprague–Dawley rat model. These results revealed that CHR protects against DOX-induced cardiotoxicity by suppressing cellular PARylation and provided critical evidence that PARylation may be a novel target for DOX-induced cardiomyopathy.

1. Introduction

Doxorubicin (DOX, also called adriamycin, ADR) belongs to anthracyclines, and is one of the most resultful chemotherapeutic agents available against various tumors such as leukaemia, breast cancer and lymphomas[1]. Unfortunately, the clinical application of DOX is largely restricted due to its serious cardiotoxicity[1–4]. The characteristic features of DOX-induced cardiac damage are the increased production of reactive oxygen species (ROS), cardiomyocyte apoptosis, the impairment of energy metabolism and mitochondrial dysfunction[5–9]. We previously reported that the DOX-elevated cytosolic α-enolase led to cardiomyocyte apoptosis and mitochondrial damage while mitochondria-located α-enolase prevent Ca^{2+}-stressed mitochondrial membrane depolarization and permeabilization[10,11]. Several antioxidants, such as vitamin E[12], *N*-acetyl cysteine[13,14], resveratrol[15] and 7-monohydroxyethylrutoside[16], were identified to relieve DOX-induced cardiomyopathy. However, it is still far from satisfaction due to the limited efficacy of these medicines on DOX-cardiomyopathy. Therefore, there is an urgent need to identify new agents to overcoming DOX-cardiomyopathy.

Chrysophanol (CHR, also known as chrysophanic acid, 1,8-dihydroxy-3-methyl-anthraquinone) is an anthraquinone compound isolated from the rhizome of *Rheum palmatum* L. It has been reported that CHR affects a wide range of biological processes, including tumour-suppression[17–20], virucidal activity[21], neuroprotection[22–26], antiplatelet and anticoagulant[27], protection from diabetes[28], inflammatory responses[23,24,26,29,30], hepatic and pulmonary injury[30,31]. The extract of *R. plamatum* and *Rheum undulatum* has protective effect on cardiovascular diseases, including cardiac infarction, myocarditis and atherosclerosis[32–34]. *Rheum turkestanicum* inhibited DOX-induced cardiomyocytes toxicity partly by anti-apoptotic activity in H9C2 cells[35], exerted protective effect against myocardial injury and nephropathy in diabetes by lowering the serum levels of glucose and lipids, and by inhibiting oxidative stress mediated lipid peroxidation[36]. However, there is very limited evidence for CHR's protective effects against cardiovascular disease. And the detailed role and underlying mechanisms for CHR's cardioprotection in DOX-induced cardiomyopathy have also not been evaluated.

Poly(ADP-ribose) polymerase-1 (PARP1), the founding subtype of the PARP enzyme family, attaches the polymers of ADP-ribose (PAR) to target proteins, a process called poly(ADP-ribosyl)ation (PARylation)[37]. Activated PARP1 contributes to at least 85% of total cellular PARPs catalytic activity[38]. PARP1 is an attractive antitumor target in clinical trials and its inhibitors including INO-1001, ABT888, PJ34 and AZD2281, were widely used in combination with chemotherapeutic agents including DOX[39–43]. DOX treatment caused a remarkable induction of PARylated protein levels in the cardiomyocytes[44–46]. Over-activation of PARP1 contributed to the cardiac dysfunction in DOX-cardiomyopathy[44], while inhibition of PARP1 protects against DOX-induced myocardial apoptosis and heart injury[44,47]. DOX-induced cellular PARylation levels may be implicated in the side-effect on the heart. Recently, CHR is shown to inhibit photoreceptor cell apoptosis through inhibiting PARP1 activity[48]. Therefore, we hypothesized that DOX-induced the enhanced cellular PARylation levels is critical for the side-effect on the heart.

In this study, we found that CHR protected against DOX-induced cardiotoxicity by suppressing cellular PARylation both *in vitro* and *in vivo*. CHR signigicantly suppressed DOX induced cardiac apoptosis, mitochondrial injury and cellular PARylation in H9C2 cells. Ectopic expression of PARP1 effectively blocked this CHR's cardioprotection and PARP1 inhibition significantly suppressed DOX-induced cardiomyocyte injury. In a rat model of DOX-cardiomyopathy, both CHR and 3AB significantly suppressed DOX-induced cardiac apoptosis, mitochondrial impairment and heart dysfunction. Collectively, these results suggest that CHR is a potential agent for overcoming DOX-induced cardiotoxicity.

2. Materials and methods

2.1. Chemical reagents

For cells, doxorubicin (DOX, purity 99.37%) was purchased from TargetMol (Target Molecule Corp., USA), and was dissolved in warm water to 10 mmol/L. Chrysophanol (CHR, purity 99.02%) was purchased from MCE (MedChemexpress, USA), and was diluted in warm DMSO to 20 mmol/L (Fig. 1A). 3-Aminobenzamide (3AB, also called as INO-1001, purity 98.11%) was obtained from Selleck (Selleck Chemicals, USA), and was dissolved in DMSO to 10 mmol/L. ABT888 (veliparib, purity 99.51%) was from APExBIO (APExBIO Technology, Houston, USA), and was diluted in DMSO to 10 mmol/L. All the solutions are stored at –20 °C.

For animals, DOX (purity over 98%) was purchased from Sangon (Shanghai, China), and was dissolved in sterile normal saline (NS) to 2 mg/mL. CHR (purity over 98%) was purchased from Meilune (Dalian, China), and was dissolved in 0.1% sodium carboxymethylcellulose (CMC-Na, Sangon, Shanghai, China) to 20 mg/mL. 3AB (purity over 98%) was obtained from Meilune (Dalian, China), and was dissolved in sterile NS to 20 mg/mL.

2.2. Animal model

The animal experimental procedures were approved by the Research Ethics Committee of Sun Yat-sen University (Guangzhou, China), and were conducted in accordance with the Guide for the Care and Use of Laboratory Animals (NIH Publication No. 85-23, revised 1996). The ninety male Sprague–Dawley rats (220–250 g, certification No. 44008500014426, SPF grade) were achieved from the Experimental Animal Center of Sun Yat-sen University (Guangzhou, China). After a few days, the animals were randomized assigned to

five groups (with 10 in each group): NS (as a control group), DOX (its cumulative doses were 15 mg/kg)[10,11], combined different doses of CHR (5, 20, and 40 mg/kg/day) with DOX, combined 3AB (40 mg/kg/day) with DOX.

2.3. Echocardiographic and morphometric measurements

At the end of the trial, two-dimensional-guided M-mode echocardiography was executed by a Technos MPX ultrasound system (ESAOTE, SpAESAOTE SpA, Italy)[49]. Basic hemodynamic parameters, such as ejection fraction (EF), fractional shortening (FS), end-systolic left ventricular volume (LVVs), end-diastolic left ventricular volume (LVVd), end-systolic interventricular septum (IVSs), end-diastolic interventricular septum (IVSd), left ventricular end-systolic internal diameter (LVIDs), left ventricular end-diastolic internal diameter (LVIDd), left ventricular end-systolic posterior wall thickness (LVPWs) and left ventricular end-diastolic posterior wall thickness (LVPWd) were measured. Afterwards, the SD rats were sacrificed, and their heart tissues were quickly removed out. The 5-μm-thick fresh histological cross sections of the heart tissues were fixed with paraformaldehyde (4%), and were stained with hematoxylin-eosin (HE), and Sirus red staining for morphometric measurement. The cryopreserved heart section would be submitted to further assay.

2.4. The culture of rat embryonic ventricular myoblastic H9C2 cells

Rat embryonic ventricular myocardial H9C2 cells were bought from the Cell Bank of the Chinese Academy of Sciences (CAS, Shanghai, China). The cells were incubated in DMEM (GIBCO, Invitrogen, Carlsbad, CA) with 10% fetal bovine serum (FBS), streptomycin (100 U/mL) and penicillin (100 U/mL) in a humidified atmosphere of 5% CO_2 at 37 °C.

2.5. Western blot analysis

Primary antibodies against PARP1 (rabbit, diluted 1:1000), Caspase 3 (rabbit, diluted 1:1000), BCL-2 (rabbit, diluted 1:1000), BAX (rabbit, diluted 1:1000), Cyt *c* (rabbit, diluted 1:1000) and VDAC1 (rabbit, diluted 1:1000) were purchased from Cell Signaling Technology. Primary antibodies against α-tubulin (diluted 1:5000) were from Sigma-Aldrich (St Louis, MO, USA). Antibodies against PAR (mouse, diluted 1:500) were obtained from Trevigen (Gaithersburg, MD, USA). Anti-mouse and anti-rabbit IgG peroxidase conjugated antibodies and other agents were from SAB (College Park, MD, USA). The procedure for Western blot analysis on H9C2 cells or cardiac tissues here has been previously reported[50]. The intensity of protein bands was measured by the Quantity One software (Bio-Rad, USA).

2.6. Isolation of cytosol and mitochondrial fractions of H9C2 cells or hearts

The cytosolic and mitochondrial fractions of H9C2 cells were obtained by a commercially available cytosol/mitochondria fractionation kit following the manufacturer's protocol (Beyotime, China). Proteins in the two fractions were diluted in lysis solution and were detected by immunoblotting analysis for analyzing the release of Cyt *c* from mitochondria to cytoplasm in H9C2 cells. The mitochondria of rat hearts were separated from fresh tissues *via* gradient centrifugations as previously reported[10].

2.7. In situ observation of DNA fragmentation and nuclear condensation

In situ DNA fragmentation of the heart sections was observed by a TdT-mediated dUTP nickend labeling (TUNEL) apoptosis identifying kit (Keygen Biotech, China) according to the manufacturer's protocol[11]. Nuclear condensation of H9C2 cells was evaluated *via* Hoechst 33342 staining[11]. In the heart fractions, the percentages of apoptotic cardiomyocytes were quantified as the ratio of TUNEL-labelled cells to total cells.

2.8. Determination of mitochondrial membrane potential (Δψm) and matrix swelling

Rhodamine 123 (Rh123, Sigma, USA) was dissolved with DMSO to 10 mg/mL for storage at –80 °C, tetra-methylrhodamine ethyl ester (TMRE) (Invitrogen, Molecular Probes, USA) was diluted with DMSO to 1 mmol/L for storage at –80 °C. In order to monitor Δψm, H9C2 cells were respectively loaded in 10 μg/mL Rh123 or 10 nmol/L TMRE at 37 °C for 10 min. For analysis of matrix swelling, H9C2 cells were stained with 1 μmol/L Mitotracker Red (Invitrogen, Carlsbad, CA, USA) at 37 °C for 10 min. Subsequently, the cells were replaced by DMEM without phenol red, and were photographed using EVOS FL Auto (Life Technologies, Bothell, WA, USA).

2.9. Mitochondrial respiration measurement[11]

Oxygen consumption of the separated fresh mitochondria was immediately measured by a Clark oxygen electrode (Strathkelvin Instrument, Scotland). Mitochondrial respiration was determined under the manufacturer's protocol (Genmed Scientifics Inc). The mitochondrial State III and State IV respiration rates in the closed reaction buffer were monitored, and the mitochondrial respiratory control ratio (RCR) was calculated as State III/State IV respiration rates. The mitochondrial ADP/O ratios were also detected.

2.10. Quantification of ATP content[11]

ATP concentrations of the heart tissues were detected by a firefly luciferin/luciferase-based ATP bioluminescence assay kit (Beyotime, China). The ATP contents were determined as nmol/mg protein by using Infinite M1000 multimode microplate reader (TECAN, Switzerland).

2.11. Cell viability assay

The cell viability of H9C2 cells was detected by MTS assay (Promega, USA) as described previously[50]. H9C2 cells were seeded in 96-well plates. After CHR exposure, MTS was supplemented into cell cultures and was incubated for 1 h at 37 °C. The absorbance was measured at a wavelength of 490 nm by a microplate reader (TECAN, Switzerland). Percent viability was determined as the relative absorbance of the different doses of CHR *vs* control cells.

2.12. Statistical analysis

The data were presented as the means ± SEM value. The statistical comparisons between two groups were conducted by Student's *t*-test. The statistical significance analysis among various

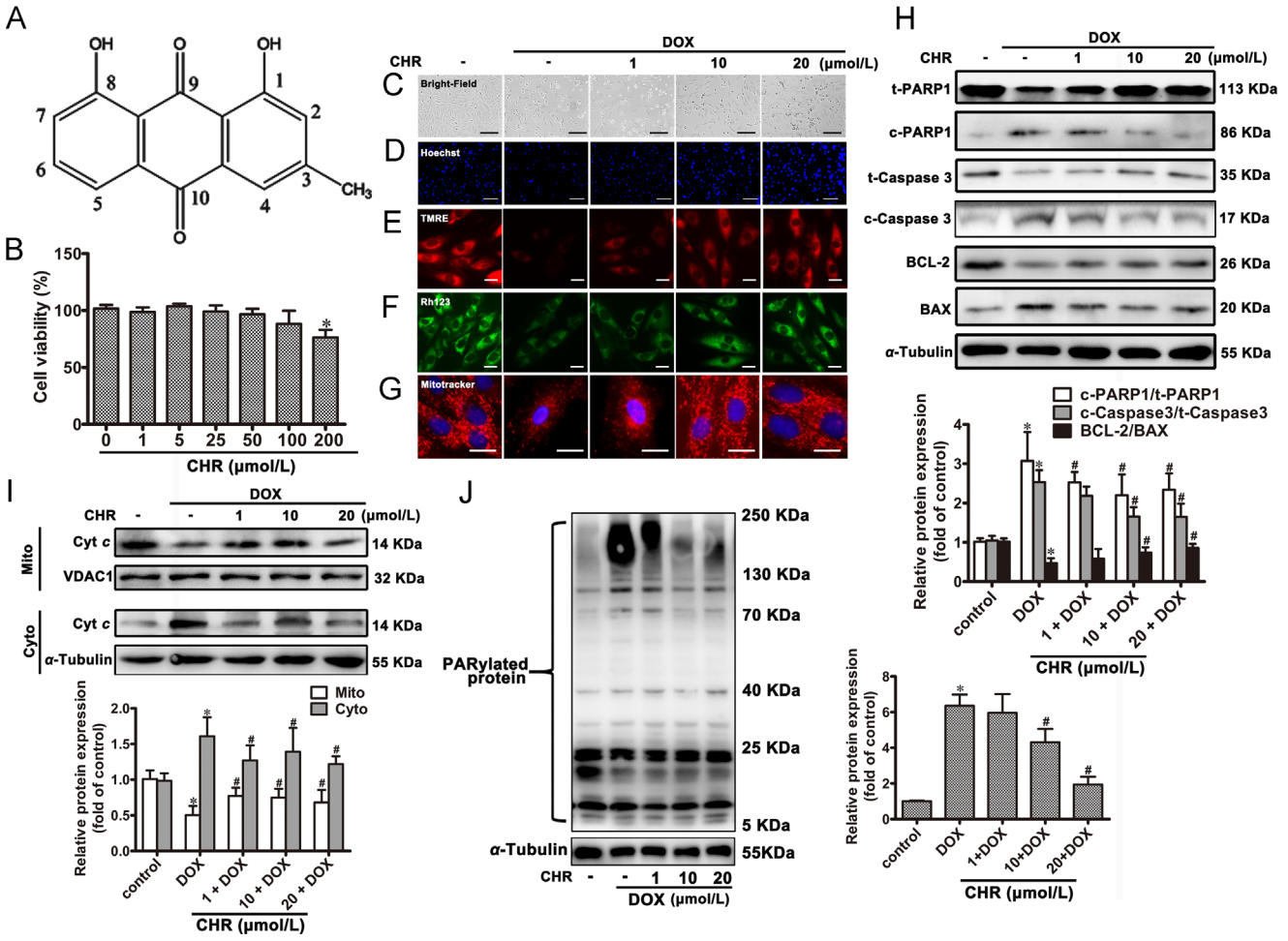

Figure 1 Chrysophanol (CHR) attenuated DOX-induced cardiomyocyte apoptosis and mitochondrial injury *in vitro*. (A) The chemical structure of CHR (1,8-dihy-droxy-3-methylanthraquinone). (B) H9C2 cells were incubated with the different doses of DOX (0, 1, 5, 25, 50, 100, and 200 μmol/L) for 12 h, and the cell viability were measured by MTS assay. H9C2 cells were pre-cultured with CHR at different doses (1, 10 and 20 μmol/L) for 12 h before stimulation with DOX (1 μmol/L). (C) The cellular morphology was observed by light microscopy. Sclae bar: 200 nm. (D) The nuclear condensation was identified by Hoechst 33342 staining. Sclae bar: 100 nm. (E)–(G) The mitochondrial membrane potential ($\Delta\psi m$) and matrix swelling was determinated using staining with TMRE, Rh123 or Mitotracker. Sclae bar: 100 nm. Representative images of five independent experiments are shown. (H) The cleavage and activation of PARP1 and caspase 3, as well as the BCL-2/BAX ratio were detected by Western blot analysis. (I) The cardiac mitochondria were isolated from H9C2 cells, and the lysed extracts were submitted to Western blot analysis to measure the release of Cyt *c* from mitochondria to cytoplasm. (J) The cardiac PARylation levels of H9C2 cells were measured by Western blot analysis. The results were normalized to those of VDAC1 or α-tubulin and were presented as the means ± SEM. $^{*}P < 0.05$ *vs*. the control group, $^{\#}P < 0.05$ *vs*. the DOX group, $n = 3$.

groups was verified by one-way analysis of variance (ANOVA) with Tukey's *post-hoc* test. In the statistical analyses, a value of $P < 0.05$ was believed statistically significant.

3. Results

3.1. CHR attenuated DOX-induced cardiomyocyte apoptosis and mitochondrial injury in vitro

DOX induces serious cardiotoxicity and irreversible cardiomyopathy in clinical application generally[1–4]. To explore the role of CHR in the process of apoptosis and mitochondrial damage by DOX, we firstly examined the cytotoxicity of CHR on rat embryonic ventricular myocardial H9C2 cells by MTS assay and found that CHR was not toxic even at high concentrations (100 μmol/L) (Fig. 1B). H9C2 cells were pre-incubated with CHR at different doses (1, 10, and 20 μmol/L) for 12 h before stimulation with DOX (1 μmol/L). CHR significantly suppressed the DOX-induced cardiomyocyte injury including the reduction of cell viability, apoptosis and nuclear condensation (Supporting Information Fig. S2A, Fig. 1C and D). In addition, we found that CHR effectively blocked DOX-induced apoptosis through inhibiting cleavage and activation of PARP1 and caspase 3, increasing BCL-2/BAX ratio (Fig. 1H) and reducing release of Cyt *c* from mitochondria to cytoplasm (Fig. 1I). To further assess the role of CHR in DOX-induced mitochondrial injury, we treated cells with CHR and DOX, results clearly showed that CHR suppressed DOX induced mitochondrial membrane depolarization and the mitochondria swelling (Fig. 1E–G). Interestingly, DOX induced PARylation in H9C2 cells were widely antagonized by CHR (Fig. 1J). Take together, our data

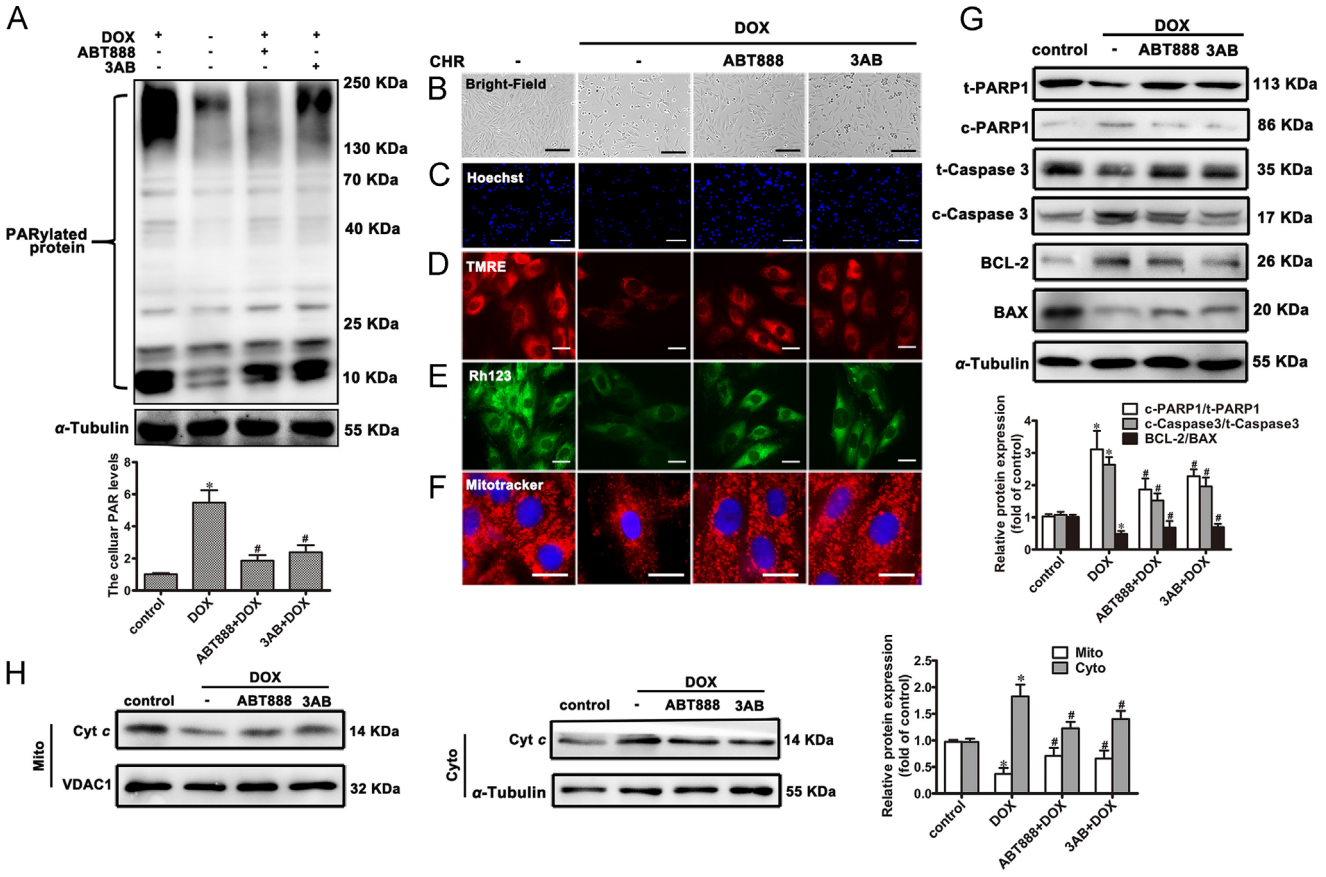

Figure 2 Inhibition of PARP1 alleviated DOX-triggered cardiomyocyte apoptosis and mitochondrial damage *in vitro*. H9C2 cells were pre-treated with the ABT888 (5 μmol/L) or 3AB (20 μmol/L) for 12 h before stimulation with DOX (1 μmol/L). (A) The cardiac PARylation levels of H9C2 cells were measured by Western blot analysis. (B) The cellular morphology was observed by light microscopy. Sclae bar: 200 nm. (C) The nuclear condensation was identified by Hoechst 33342 staining. Sclae bar: 100 nm. (D)–(F) The mitochondrial membrane potential ($\Delta\psi m$) and matrix swelling was determinated using staining with TMRE, Rh123 or Mitotracker. Sclae bar: 100 nm. Representative images of five independent experiments are shown. (G) The cardiac cleavage and activation of PARP1 and caspase 3, as well as the BCL-2/BAX ratio were detected by Western blot analysis. (H) The lysed extracts were measured by Western blot analysis to measure the release of Cyt *c* from mitochondria to cytoplasm. The results were normalized to those of α-tubulin/VDAC1 and were presented as the means ± SEM. $^{*}P < 0.05$ *vs.* the control group, $^{\#}P < 0.05$ *vs.* the DOX group, $n = 3$.

suggest that CHR exerts a clearly protective effect in DOX-induced cardiomyocyte apoptosis and mitochondrial injury *in vitro*.

3.2. *Inhibition of PARP1 alleviated DOX-triggered cardiomyocyte apoptosis and mitochondrial damage in vitro*

The prominent effect of DOX on the cellular PARylation prompted us to investigate whether PARP1 was involved in DOX-induced cardiomyocyte apoptosis and mitochondrial damage. Indeed, the cells were pre-incubated with the specific inhibitors of PARP1 (3AB and ABT888) followed by DOX for 12 h, PARP1 inhibitors suppressed DOX-induced PARylation in H9C2 cells (Fig. 2A). In addition, the apoptotic cardiomyocytes, the nuclear condensation and cell death induced by DOX was inhibited by 3AB or ABT888 (Fig. 2B, C, and Fig. S2B). Furthermore, mitochondrial membrane depolarization and swelling induced by DOX was suppressed by PARP1 inhibitors (Fig. 2D–F). PARP1 inhibitors also led to the reduced cleavage and activation of PARP1 and caspase 3, as well as the increased BCL-2/BAX ratio (Fig. 2G). The decreased protein level of Cyt *c* in the DOX-treated mitochondrial fraction was greatly reversed by PARP1 inhibitors (Fig. 2H). These results implicate that the inhibition of PARP1 catalytic activity, to some extent, protects against DOX-induced cardiomyocyte apoptosis and mitochondrial injury.

3.3. *The cellular PARylation was involved in the protection of CHR on DOX-induced cardiotoxicity in vitro*

Over-activation of PARP1 exerts a critical effect on the cardiac dysfunction in DOX-cardiomyopathy[44]. Previous reports showed that CHR suppressed photoreceptor cell cleavage of PARP1 and caspase 3 in an *N*-methyl-*N*-nitrosourea-induced mouse apoptosis model of retinal degeneration[48]. We then examined whether PARP1 was involved in the protective effect of CHR on DOX-induced cardiomyocyte apoptosis and mitochondrial dysfunction. We ectopically expressed PARP1 or GFP control in H9C2 cells by infected with adenovirus Ad-PARP1 or Ad-GFP (Fig. 3A–G, and Fig. S2C). The overexpressed PARP1 resulted in the cardiomyocyte impairments and obvious mitochondrial dysfunction, indicating that PARP1 overexpression could be as a

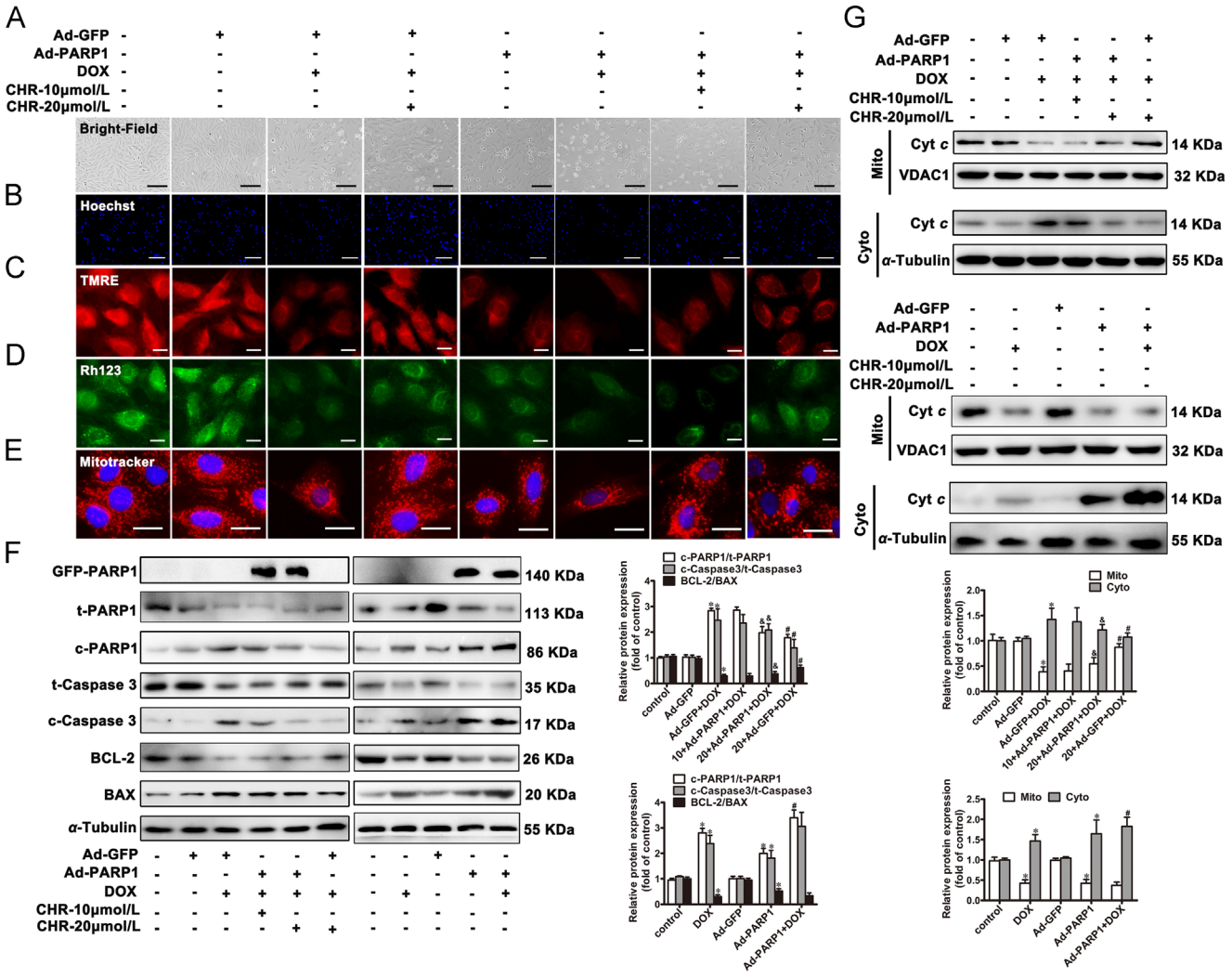

Figure 3 PARP1 was involved in the protection of CHR on DOX-induced cardiotoxicity *in vitro*. H9C2 cells were pre-infected with Ad-PARP1 or Ad-GFP followed by CHR (10 and 20 μmol/L) incubation with or without DOX. (A) The cellular morphology was observed by light microscopy. Sclae bar: 200 nm. (B) The nuclear condensation was identified by Hoechst 33342 staining. Sclae bar: 100 nm. (C)–(E) The mitochondrial membrane potential ($\Delta\psi m$) and matrix swelling was determined using staining with TMRE, Rh123 or Mitotracker. Sclae bar: 100 nm. Representative images of five independent experiments are shown. (F) The cleavage and activation of PARP1 and caspase 3, as well as the BCL-2/BAX ratio were determined by Western blot analysis. (G) The cardiac mitochondria were isolated from H9C2 cells, and the lysed extracts were submitted to Western blot analysis to detect the release of Cyt *c* from mitochondria to cytoplasm. The results were normalized to those of VDAC1 or *α*-tubulin and were presented as the means ± SEM. $^{*}P < 0.05$ *vs.* the control group, $^{\#}P < 0.05$ *vs.* the Ad-GFP+DOX group, $^{\&}P < 0.05$ *vs.* the 20+Ad-GFP+DOX group, $n = 3$.

model of cardiomyocyte injury. The effect was further aggravated upon DOX stimulation. CHR protected against DOX-induced cardiac apoptosis and mitochondrial damage in control cells while ectopic expression of PARP1 effectively blocked this CHR's cardioprotection (Fig. 3A–E, and Fig. S2C). In addition, the inhibitory effects of CHR on DOX-induced cardiomyocyte apoptosis and mitochondrial injury were attenuated by adenovirus-mediated PARP1 overexpression, as shown by increased the cleavage and activation of PARP1 and caspase 3, and the decreased BCL-2/BAX ratio, as well as the elevated release of Cyt *c* from mitochondria to cytoplasm (Fig. 3F and G). These results indicate that CHR protected against DOX-stimulated cardiotoxicity at least partially *via* inhibiting cellular PARylation levels.

3.4. CHR and 3AB both protected against DOX-induced heart injury in SD rats

Given the effective role of CHR protecting against DOX-stimulated cardiotoxicity, we examined whether CHR possesses any protection against DOX-induced heart injury in SD rats. SD rats were intraperitoneally injected with a cumulative dose of 15 mg/kg DOX by three equal injections (on days 1, 6 and 11, respectively) for 15 days[10,11]. To explore the effects of CHR or 3AB (a PARP1 inhibitor) on the cardiac function of DOX-induced rats, the different doses of CHR (Low: 5 mg/kg/day; Medium: 20 mg/kg/day; High: 40 mg/kg/day) or 3AB (40 mg/kg/day) were intragastrically or intraperitoneally treated to SD rats one time every day for 7 days before DOX administration. Control group

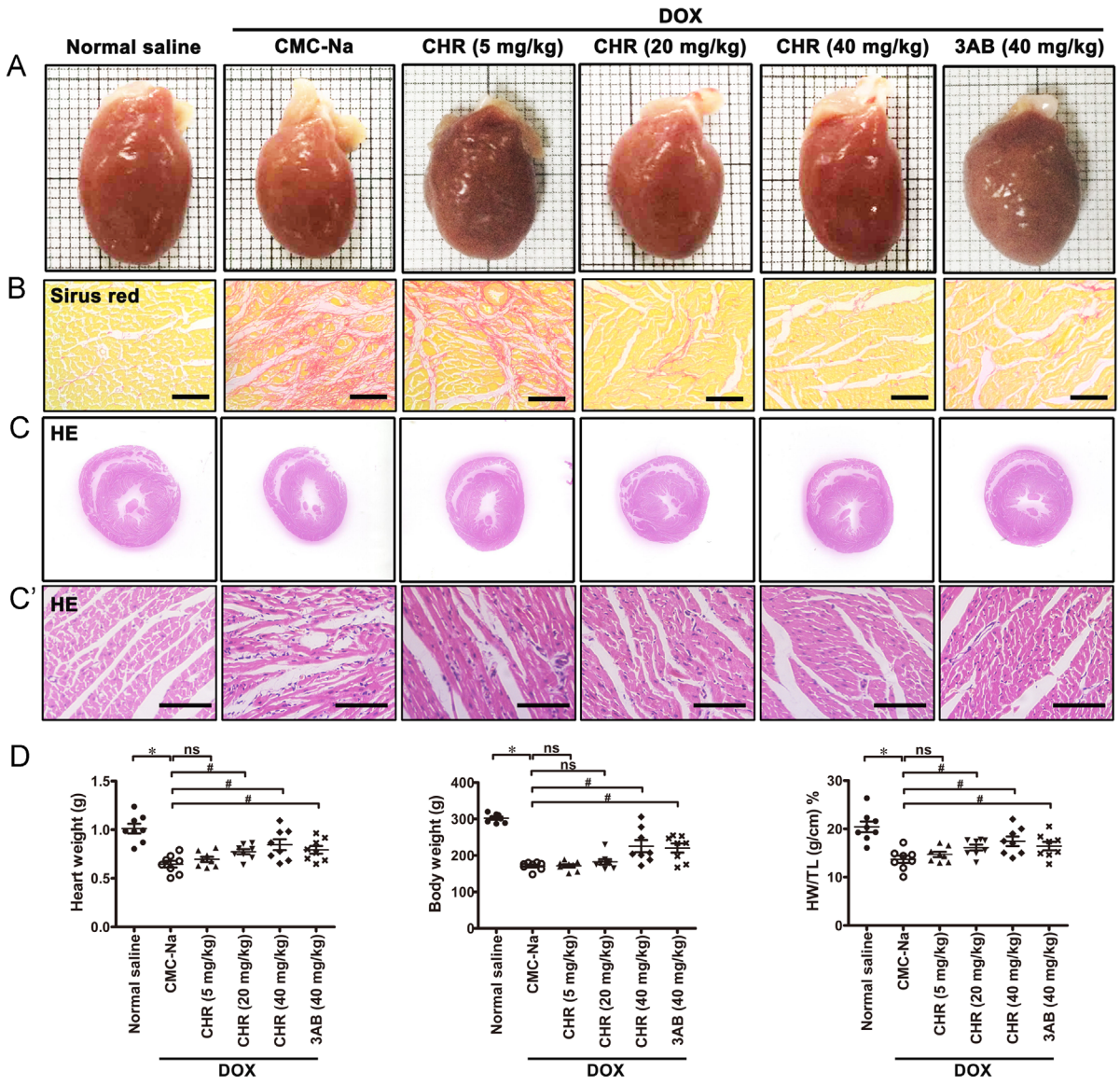

Figure 4 Both Chrysophanol (CHR) and 3-aminobenzamide (3AB) protected against DOX-induced heart injury in Sprague–Dawley (SD) rats. SD rats were intragastrically treated with different doses of CHR (5, 20, and 40 mg/kg/day) or intraperitoneally injected with 3AB (40 mg/kg/day) for 7 days followed by DOX intraperitoneal injection (its cumulative doses were 15 mg/kg by three equal injections for 15 days) or an equal volume of sterile normal saline/sodium carboxymethylcellulose (CMC-Na). (A)–(C) Gross hearts, Sirus red and HE-stained transections of the left ventricle. Sclae bar: 100 nm. (D)–(F) The heart weight (HW), the body weight (BW), as well as the heart weight to the tibia length (HW/TL) ratios were calculated. The results were attended as the means ± SEM. $^{*}P < 0.05$ *vs*. Normal saline group, $^{\#}P < 0.05$ *vs*. the DOX group, $n = 10$. ns: no statistical difference.

were treated with the vehicle in an equal volume of CMC-Na. Results showed that the hearts from DOX-treated rats were distinctly smaller than those from control rats (Fig. 4A), and also presented apparent myocardial fibrosis and inflammatory cell infiltration *via* Sirus red and HE staining (Fig. 4B–C). In addition, the heart weight (HW, Fig. 4D), the body weight (BW, Fig. 4E), tibia length (TL) (Supporting Information Fig. S3B) and the heart weight to the tibia length (HW/TL ratio, Fig. 4F) in DOX-rats were decreased, the heart weight to the body weight (HW/BW) ratios were enhanced (Fig. S3A). Meanwhile, echocardiographic analysis (Fig. 5) exhibited that the ejection fraction (EF%, Fig. 5B), fractional shortening (FS%, Fig. 5C), cardiac output (CO, Fig. 5D), interventricular septum (IVS, Fig. 5F), left ventricular diameter (LVID, Fig. 5G), left ventricular volume (LVV, Fig. 5H) and left ventricular posterior wall thickness (LVPW, Fig. 5I) were reduced, while heart rates (HR, Fig. 5E) was unaltered in the hearts of DOX-injected rats. These data reveal that the cardiotoxicity model induced by DOX was successful established *in vivo*.

CHR (5, 20, and 40 mg/kg/day) dose-dependently attenuated the myocardiopathy responses triggered by DOX, as indicated by the augmented morphologic characteristics, LVID, IVS, LVPW and HW/TL, as well as heart function (including EF, FS and CO) (Figs. 4 and 5). The high doses of CHR (40 mg/kg/day) displayed significant protective effect on the heart function of DOX treatment (Figs. 4 and 5). Similarly, the levels of myocardial fibrosis (Fig. 4B) and inflammatory cell infiltrates (Fig. 4C and C') were distinctly declined, HW (Fig. 4D), BW (Fig. 4E), TL

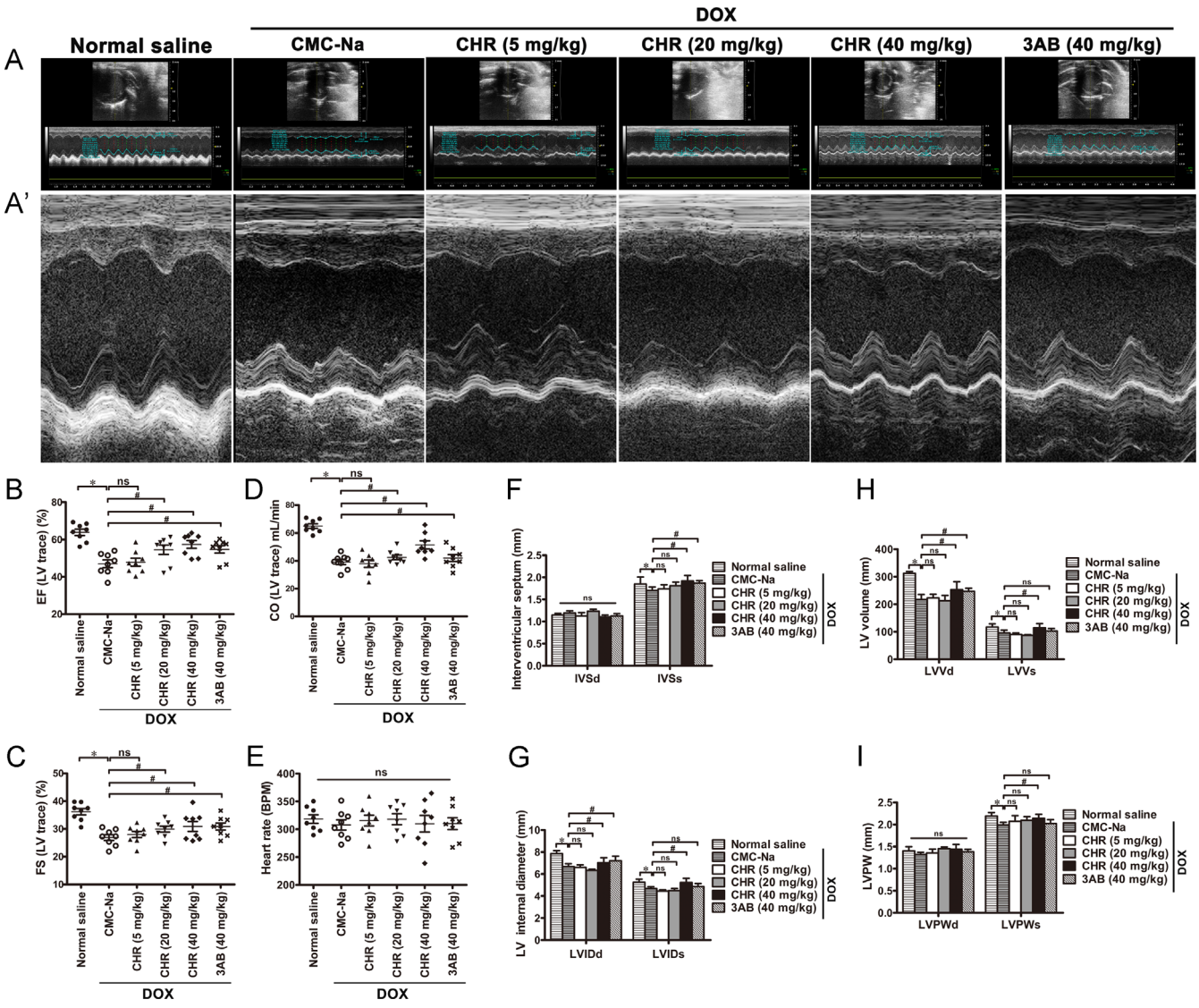

Figure 5 Both Chrysophanol (CHR) and 3-aminobenzamide (3AB) relieved DOX-induced heart dysfunction of Sprague–Dawley (SD) rats. SD rats were intragastrically treated with different doses of CHR (5, 20, and 40 mg/kg/day) or intraperitoneally injected with 3AB (40 mg/kg/day) for 7 days followed by DOX intraperitoneal injection (its cumulative doses were 15 mg/kg by three equal injections for 15 days) or an equal volume of sterile normal saline/sodium carboxymethylcellulose (CMC-Na). (A) and (A') The representative echocardiographic graphs are presented. (B)–(I) The echocardiographic parameters were measured, including the ejection fraction (EF), fractional shortening (FS), cardiac output (CO), heart rates (HR), interventricular septum (IVS), left ventricular diameter (LVID), left ventricular volume (LVV) and left ventricular posterior wall thickness (LVPW). The results were attended as the means ± SEM. $^{*}P < 0.05$ *vs*. Normal saline group, $^{\#}P < 0.05$ *vs*. the DOX group, $n = 10$. ns: no statistical difference.

(Fig. S3B), HW/TL (Fig. 4F) and echocardiographic parameters (Fig. 5) were largely improved after 40 mg/kg/day 3AB pre-injection. The alteration of HR (Fig. 5E) and LVPW (Fig. 5I) remained rather obscure. Take together, our data suggest that both CHR and 3AB effectively protect against DOX-induced heart injury in SD rats.

3.5. *CHR overcomed DOX-induced cardiomyocyte apoptosis and mitochondrial dysfunction in SD rats*

It is well documented that DOX rapidly induced cardiomyocyte apoptosis and mitochondrial dysfunction[1–4]. Our results showed that DOX induced the obvious cardiac apoptosis and energy imbalance in SD rats. The sections of rat hearts were stained with TUNEL labeling and were subsequently examined by light microscopy (Fig. 6A), and the lysed extracts were submitted to Western blot analysis (Fig. 6B). Compared with the control hearts (only about 2%), the percentages of TUNEL-positive cells were significantly increased (over 15%) after DOX treatment (Fig. 6A). Additionally, DOX administration accelerated the cleavage and activation of PARP1 or caspase 3, as well as restrained the BCL-2/BAX ratio (Fig. 6B). Meanwhile, cardiac mitochondrial respiration of SD rats was detected through measuring oxygen consumption of isolated fresh mitochondria by a Clark oxygen electrode. As shown in Fig. 7A–D, state III respiration, RCR and ADP/O was respectively increased to about 115 nmol O/mg/min, 3.1 and 1.15, meanwhile little effect on state IV respiration upon DOX treatment. Furthermore, DOX resulted in the declined ATP content of

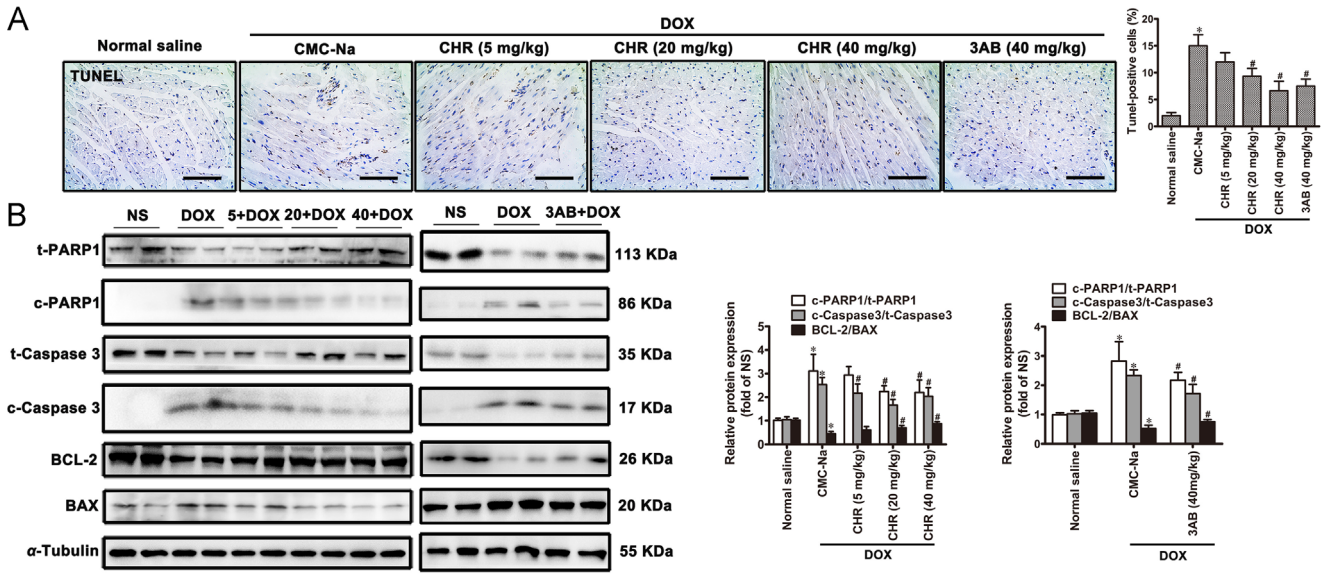

Figure 6 Both Chrysophanol (CHR) and 3-aminobenzamide (3AB) relieved DOX-induced cardiac apoptosis of Sprague–Dawley (SD) rats. SD rats were intragastrically treated with different doses of CHR (5, 20, and 40 mg/kg/day) or intraperitoneally injected with 3AB (40 mg/kg/day) for 7 days followed by DOX intraperitoneal injection (its cumulative doses were 15 mg/kg by three equal injections for 15 days) or an equal volume of sterile normal saline/sodium carboxymethylcellulose (CMC-Na). (A) The sections of rat heart were stained with TUNEL labeling, were observed by light microscopy. Representative images of five independent experiments are shown. Sclae bar: 100 nm. (B) The lysed extracts were detected the apoptotic protein levels, such as the protein cleavage and activation of PARP1 or caspase 3, as well as the BCL-2/BAX ratio. The results were presented as the means ± SEM. $^{*}P < 0.05$ *vs*. Normal saline group, $^{\#}P < 0.05$ *vs*. the DOX group, $n = 10$. ns: no statistical difference.

rat hearts, the vast majority of which is produced *via* mitochondrial respiration (Fig. 7E). The heart PARylation levels of SD rats after DOX treatment were widely activated (Fig. 7F).

The different dosages of CHR or 3AB (40 mg/kg/day) protected myocardium cells against DOX-apoptosis, as implied by the dropped TUNEL-labeling apoptosis rates (5 mg/kg/day: 12%; 20 mg/kg/day: 9%; 40 mg/kg/day: 7%) (Fig. 6A), as well as the reduced cleavage and activation of protein PARP1, caspase 3 and the raised BCL-2/BAX ratio (Fig. 6B). To explore the effect of CHR or 3AB on the DOX-stressed energy imbalance, the mitochondrial oxidative phosphorylation and ATP generation was tested. Fig. 7A–E showed that the respiration impairment in cardiac mitochondria was highly ameliorated, the reduced of ATP level in DOX-rat hearts was partially reversed by CHR or 3AB pretreatment. The induced effect of DOX on the heart PARylation levels was significantly surpressed by CHR or 3AB (Fig. 7F). These data suggest that both CHR and 3AB inhibited DOX-induced cardiomyocyte apoptosis and mitochondrial dysfunction *in vivo*.

4. Discussion

DOX is one of the highly effective chemotherapeutic anthracyclines available against a broad spectrum of tumors including leukaemia, breast cancer and lymphomas[1]. But the clinical application of DOX is restricted due to its unintended risk of cardiotoxicity and irreversible cardiomyopathy[1–4]. It is characterized by excessive formation of ROS, cardiomyocyte apoptosis, the impairment of energy metabolism and mitochondrial dysfunction[5–9]. Currently, several antioxidants, such as vitamin E[12], *N*-acetyl cysteine[13,14], resveratrol[15] and 7-monohydroxyethylrutoside[16], were identified to process protection against DOX-induced cardiotoxicity. However, these agents failed to improve the heart symptoms in clinical trials or in animal models suffering DOX-cardiomyopathy, it is urgent to identify novel drugs or targets to overcoming DOX-induced cardiotoxicity. Here, we present several lines of evidence that CHR may be a new potential agent for protection against DOX-induced cardiotoxicity. CHR signigicantly suppressed DOX induced cardiac apoptosis, mitochondrial injury and cellular PARylation in H9C2 cells. Ectopic expression of PARP1 effectively blocked this CHR's cardioprotection and PARP1 inhibition significantly suppressed DOX-induced cardiomyocyte injury. Pre-administration with CHR or 3AB both relieved DOX-caused cardiac apoptosis, mitochondrial impairment and heart dysfunction in SD rat model. In summary, we found that the cellular PARylation was associated with the protection of CHR from DOX-cardiotoxicity.

CHR, a natural anthraquinone compound isolated from Rhubarb, the rhizome of *R. palmatum* L., plays an important role in the multiple biological processes, including tumour-suppression, virucidal activity, antiplatelet and anticoagulant, protection from cerebral ischemia/reperfusion, diabetes, inflammatory responses, hepatic and pulmonary injury[17–31]. Mechanistically, CHR induces the ROS production and impairment of mitochondrial ATP synthesis, resulting in tumor necrosis in human liver cancer cells or in human lung cancer A549 Cells[18–20]. In addition, CHR inhibites the proliferation of colon cancer cells *via* suppressing EGFR/mTOR signaling pathway[17]. Besides, the neuroprotection effect of CHR has been proved in a few models, such as the cerebral ischemia-reperfusion injury (through reduced caspase 3 expression and NALP3 inflammasome activation)[22,23], radical-mediated oxidative damage in BV2 murine microglia[24], lead exposure-induced injury model[25] and lipopolysaccharide-induced depression targeting P2X7[26]. Furthermore, the anti-inflammatory activity mediated by CHR relieves paraquat-stressed lung injury through activating peroxisome proliferator-activated receptors (PPARs), LPS/D-GalN-caused hepatic injury by inhibiting the RIP140/NF-κB pathway, as well as dextran sulfate sodium-induced colitis *via* the suppressing of NF-κB/Caspase-1 activation[29–31].

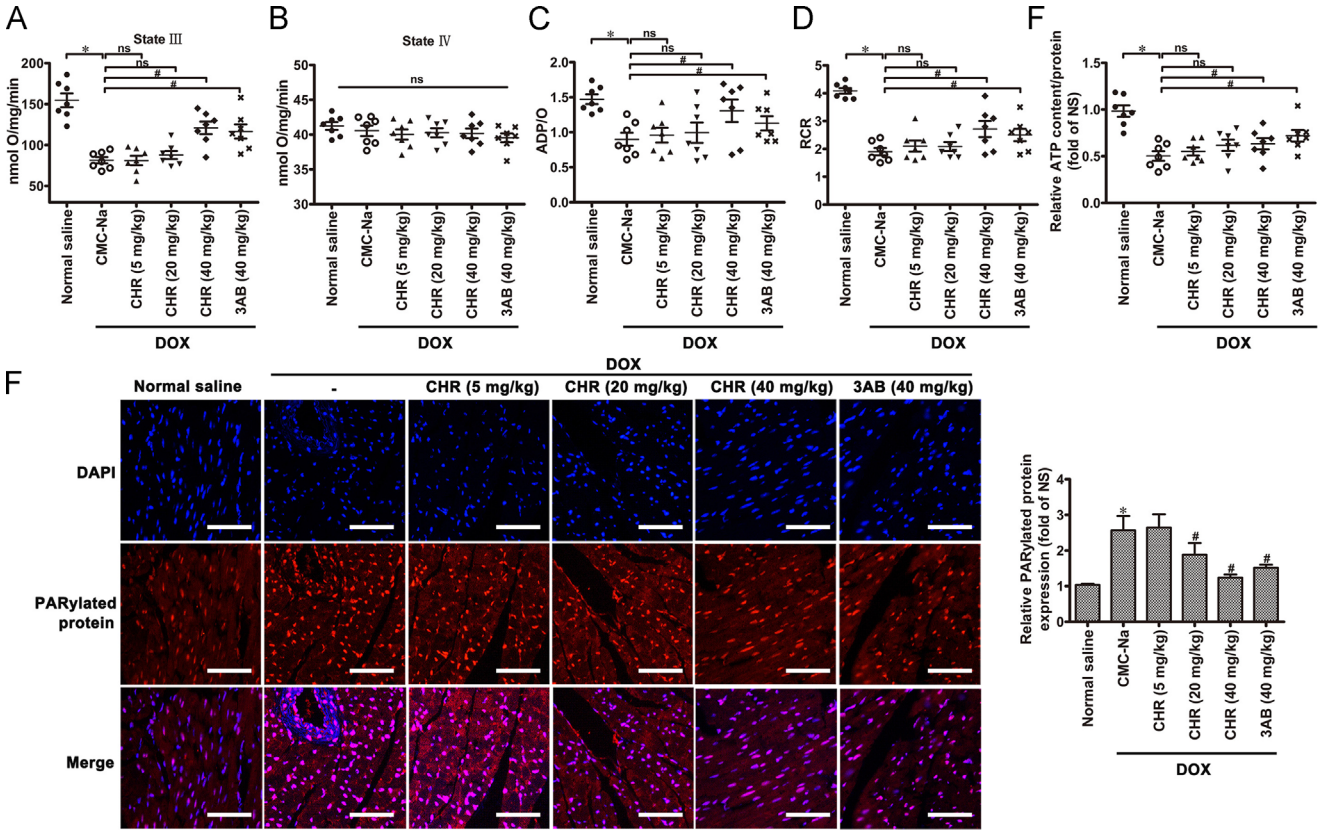

Figure 7 Chrysophanol (CHR) and 3-aminobenzamide (3AB) both relieved DOX- induced mitochondrial dysfunction of Sprague–Dawley (SD) rats. SD rats were intragastrically treated with different doses of CHR (5, 20, and 40 mg/kg/day) or intraperitoneally injected with 3AB (40 mg/kg/day) for 7 days followed by DOX intraperitoneal injection (its cumulative doses were 15 mg/kg by three equal injections for 15 days) or an equal volume of sterile normal saline/sodium carboxymethylcellulose (CMC-Na). (A)–(E) The rat heart state III and IV respiration, the heart respiratory control ratio (RCR), ADP/O and ATP content was respectively determined. (F) The heart PARylation levels of SD rats were photographed using EVOS FL Auto. Representative images of five independent experiments are shown. $^{*}P < 0.05$ *vs*. Normal saline group, $^{\#}P < 0.05$ *vs.* the DOX group, $n = 10$. ns: no statistical difference.

It has been reported that the extract of *R. plamatum* and *R. undulatum* processes protective effect on cardiovascular diseases, including cardiac infarction, myocarditis and atherosclerosis[32–34]. For instance, emodin (1,3,8-trihydroxy-6-methylanthraquinone), an anthraquinone compound extracted mainly from the root and rhizome of *R. palmatum*, mitigated autoimmune or viral myocarditis through inhibiting inflammation and autoimmunity, as well as reduced the myocardial infarct size[32,33]. Lai Fu Cheng Qi decoction (consisting of *R. palmatum* L.) was shown to exert a protective effect on severe acute pancreatitis-induced myocardial injury in rats[34]. Besides, *R. turkestanicum* inhibited DOX-induced cardiomyocytes toxicity partly by anti-apoptotic activity in H9C2 cells[35], exerted protective effect against myocardial injury and nephropathy in diabetes by lowering the serum levels of glucose and lipids, and by inhibiting oxidative stress mediated lipid peroxidation[36]. Rhaponticin from Rhubarb rhizomes alleviates liver steatosis and improves blood glucose and lipid profiles in KK/Ay diabetic mice[51]. However, whether CHR may protect against cardiovascular disease remained to be explored.

Upon DNA single and/or double-strand breakages, or oxygen/nitrogen-derived free radical injury, PARP1 (responsible for at least 85% of total cellular PARPs catalytic activity) is highly activated and catalyzes the process of PARylated modification[38]. PARP1 is an attractive antitumor target and its inhibitors such as INO-1001, ABT888, PJ34 and AZD2281 were extensively used in combination with chemotherapeutic agents including DOX in clinical trials[39–43]. Numerous studies have noticed that PJ34 combining with DOX treatment could improve endogenous topoisomerase IIa protein, finally leading to cell death in HeLa cells[39]. The inhibition of PARP1 regulates snail expression at transcriptional level, suppresses Snail/LSD1-mediated PTEN and chemosensitizes cancer cells in the DOX-exposed cells[40,41]. The inhibitor of PARP1 (INO-1001) has the capacity to enhance DOX-anti-tumor effect in p53 deficient breast cancer[43].

In the heart, activation of PARP1 contributes to the various cardiovascular diseases, which were accompanied by the increased PARylated-target proteins, NAD repletion and sirtuins inactivation[44–47,52–54]. Previous papers from our laboratory demonstrated that PARP1 is strongly activated by AngII or isoproterenol (ISO), meanwhile its novel inhibitors (salvianolic acid B and AG-690/11026014) protect the myocardium from Ang II-stressed hypertrophy *in vitro* and *in vivo*[55–58]. Recently, we have reported that the increased PARylation level of FoxO3 play a crucial role in ISO-caused cardiac hypertrophy *in vivo* and *in vitro*[37]. Over-activation of PARP1 exerts a critical effect on the cardiac dysfunction in DOX-cardiomyopathy[44]. The PARylated protein levels were dramatically induced by DOX in the cardiomyocytes[44–47]. Inhibition of PARP protects against DOX-induced myocardial apoptosis and heart injury[44,47]. Hence, DOX-induced

the enhanced cellular PARylation levels may be implicated in its side-effect on heart.

Here, we found the rat myocardium or myocardial H9C2 cells contained high PARylated-target proteins after DOX treatment. In the PARP1-overexpressing H9C2 cells, the DOX-induced cardiomyocyte apoptosis and mitochondrial injury could not be relieved by CHR treatment. Moreover, the inactivated PARP1 (by its inhibitors) attenuated DOX-induced heart injury, cardiomyocyte apoptosis and mitochondrial dysfunction *in vivo* and *in vitro*.

In current research, our results clearly identified CHR as a new potential agent which may effectively protect against DOX-induced cardiotoxicity through decreasing DOX-induced cellular PARylation *in vivo* and *in vitro*. Our findings here may have immediate implications on the development of a new therapeutic strategy for overcoming DOX-induced cardiotoxicity.

The clinical application of doxorubicin in cancer chemotherapy is restricted by its severe cardiotoxic effects. The major findings in this study are of significant importance and provide new insights into the mechanism for CHR protection against DOX-induced cardiotoxicity by suppresses cellular PARylation. Further studies are required to explore the exact role of CHR in the cardiac PARylated protein. Moreover, whether the combination of CHR with DOX potentiates the anti-tumor effect and its related potential mechanism needs to be further investigated.

Acknowledgments

This research was supported by grants from the 111 Project (No. B16047, China), National Natural Science Foundation of China (81473205, 81673433, 81803521, and 81872860), Major Project of Platform Construction Education Department of Guangdong Province (No. 2014GKPT002, China), and Special Program for Applied Science and Technology of Guangdong Province (Nos. 2015B020232009, 2014B020210003 and 2013B090700010, China), National Engineering and Technology Research Center for New drug Druggability Evaluation (Seed Program of Guangdong Province, 2017B090903004, China), Guangzhou Science and Technology Program Project (No. 201604020121, China), Medical Scientific Research Foundation of Guangdong Province (No. A2018078, China).

Appendix A. Supporting information

Supporting data associated with this article can be found in the online version at https://doi.org/10.1016/j.apsb.2018.10.008.

References

1. Li LH, Takemura G, Li YW, Miyata S, Esaki M, Okada H, et al. Preventive effect of erythropoietin on cardiac dysfunction in doxorubicin-induced cardiomyopathy. *Circulation* 2006;**113**:535–43.
2. Miyagawa K, Emoto N, Widyantoro B, Nakayama K, Yagi K, Rikitake Y, et al. Attenuation of doxorubicin-induced cardiomyopathy by endothelin-converting enzyme-1 ablation through prevention of mitochondrial biogenesis impairment. *Hypertension* 2010;**55**:738–46.
3. Schwebe M, Ameling S, Hammer E, Monzel JV, Bonitz K, Budde S, et al. Protective effects of endothelin receptor A and B inhibitors against doxorubicin-induced cardiomyopathy. *Biochem Pharmacol* 2015;**94**:109–29.
4. Koh JS, Yi CO, Heo RW, Ahn JW, Park JR, Lee JE, et al. Protective effect of cilostazol against doxorubicin-induced cardiomyopathy in mice. *Free Radic Biol Med* 2015;**89**:54–61.
5. Sterba M, Popelova O, Vavrova A, Jirkovsky E, Kovarikova P, Gersl V, et al. Oxidative stress, redox signaling, and metal chelation in anthracycline cardiotoxicity and pharmacological cardioprotection. *Antioxid Redox Signal* 2013;**18**:899–929.
6. Zhou S, Starkov A, Froberg MK, Leino RL, Wallace KB. Cumulative and irreversible cardiac mitochondrial dysfunction induced by doxorubicin. *Cancer Res* 2001;**61**:771–7.
7. Green PS, Leeuwenburgh C. Mitochondrial dysfunction is an early indicator of doxorubicin-induced apoptosis. *Biochim Biophys Acta* 2002;**1588**:94–101.
8. Umanskaya A, Santulli G, Xie W, Andersson DC, Reiken SR, Marks AR. Genetically enhancing mitochondrial antioxidant activity improves muscle function in aging. *Proc Natl Acad Sci U S A* 2014;**111**:15250–5.
9. Santulli G, Xie W, Reiken SR, Marks AR. Mitochondrial calcium overload is a key determinant in heart failure. *Proc Natl Acad Sci U S A* 2015;**112**:11389–94.
10. Gao S, Li H, Cai Y, Ye JT, Liu ZP, Lu J, et al. Mitochondrial binding of α-enolase stabilizes mitochondrial membrane: its role in doxorubicin-induced cardiomyocyte apoptosis. *Arch Biochem Biophys* 2014;**542**:46–55.
11. Gao S, Li H, Feng XJ, Li M, Liu ZP, Cai Y, et al. α-Enolase plays a catalytically independent role in doxorubicin-induced cardiomyocyte apoptosis and mitochondrial dysfunction. *J Mol Cell Cardiol* 2015;**79**:92–103.
12. Berthiaume JM, Oliveira PJ, Fariss MW, Wallace KB. Dietary vitamin E decreases doxorubicin-induced oxidative stress without preventing mitochondrial dysfunction. *Cardiovasc Toxicol* 2005;**5**:257–67.
13. Dresdale AR, Barr LH, Bonow RO, Mathisen DJ, Myers CE, Schwartz DE, et al. Prospective randomized study of the role of *N*-acetyl cysteine in reversing doxorubicin-induced cardiomyopathy. *Am J Clin Oncol* 1982;**5**:657–63.
14. Myers C, Bonow R, Palmeri S, Jenkins J, Corden B, Locker G, et al. A randomized controlled trial assessing the prevention of doxorubicin cardiomyopathy by *N*-acetylcysteine. *Semi Oncol* 1983;**10**:53–5.
15. Tatlidede E, Sehirli O, Velioglu-Ogunc A, Cetinel S, Yegen BC, Yarat A, et al. Resveratrol treatment protects against doxorubicin-induced cardiotoxicity by alleviating oxidative damage. *Free Radic Res* 2009;**43**:195–205.
16. Bruynzeel AM, Niessen HW, Bronzwaer JG, van der Hoeven JJ, Berkhof J, Bast A, et al. The effect of monohydroxyethylrutoside on doxorubicin-induced cardiotoxicity in patients treated for metastatic cancer in a phase II study. *Br J Cancer* 2007;**97**:1084–9.
17. Lee MS, Cha EY, Sul JY, Song IS, Kim JY. Chrysophanic acid blocks proliferation of colon cancer cells by inhibiting EGFR/mTOR pathway. *Phytother Res* 2011;**25**:833–7.
18. Ni CH, Chen PY, Lu HF, Yang JS, Huang HY, Wu SH, et al. Chrysophanol-induced necrotic-like cell death through an impaired mitochondrial ATP synthesis in Hep3B human liver cancer cells. *Arch Pharm Res* 2012;**35**:887–95.
19. Lu CC, Yang JS, Huang AC, Hsia TC, Chou ST, Kuo CL, et al. Chrysophanol induces necrosis through the production of ROS and alteration of ATP levels in J5 human liver cancer cells. *Mol Nutr Food Res* 2010;**54**:967–76.
20. Ni CH, Yu CS, Lu HF, Yang JS, Huang HY, Chen PY, et al. Chrysophanol-induced cell death (necrosis) in human lung cancer A549 cells is mediated through increasing reactive oxygen species and decreasing the level of mitochondrial membrane potential. *Environ Toxicol* 2014;**29**:740–9.
21. Semple SJ, Pyke SM, Reynolds GD, Flower RLP. *In vitro* antiviral activity of the anthraquinone chrysophanic acid against poliovirus. *Antivir Res* 2001;**49**:169–78.
22. Yan J, Zheng MD, Zhang DS. Chrysophanol liposomes protects brain against cerebral ischemia–reperfusion injury by reducing expression of caspase 3 in mice. *Lat Am J Pharm* 2014;**33**:973–81.
23. Zhang N, Zhang XJ, Liu XX, Wang H, Xue J, Yu JY, et al. Chrysophanol inhibits NALP3 inflammasome activation and ameliorates cerebral ischemia/reperfusion in mice. *Mediat Inflamm* 2014:370530.

24. Lin FQ, Zhang C, Chen XZ, Song E, Sun SY, Chen MH, et al. Chrysophanol affords neuroprotection against microglial activation and free radical-mediated oxidative damage in BV2 murine microglia. *Int J Clin Exp Med* 2015;**8**:3447–55.
25. Zhang J, Yan CL, Wang S, Hou Y, Xue GP, Zhang L. Chrysophanol attenuates lead exposure-induced injury to hippocampal neurons in neonatal mice. *Neural Regen Res* 2014;**9**:924–30.
26. Zhang K, Liu JY, You XT, Kong P, Song YC, Cao L, et al. P2X7 as a new target for chrysophanol to treat lipopolysaccharide-induced depression in mice. *Neurosci Lett* 2016;**613**:60–5.
27. Seo EJ, Ngoc TM, Lee SM, Kim YS, Jung YS. Chrysophanol-8-*O*-glucoside, an anthraquinone derivative in rhubarb, has antiplatelet and anticoagulant activities. *J Pharmacol Sci* 2012;**118**:245–54.
28. Lee MS, Sohn CB. Anti-diabetic properties of chrysophanol and its glucoside from Rhubarb Rhizome. *Biol Pharm Bull* 2008;**31**:2154–7.
29. Kim SJ, Kim MC, Lee BJ, Park DH, Hong SH, Um JY. Anti-inflammatory activity of chrysophanol through the suppression of NF-kappa B/caspase-1 activation *in vitro* and *in vivo*. *Molecules* 2010;**15**:6436–51.
30. Li A, Liu YG, Zhai L, Wang LY, Lin Z, Wang SM. Activating peroxisome proliferator-activated receptors (PPARs): a new sight for chrysophanol to treat paraquat-induced lung injury. *Inflammation* 2016;**39**:928–37.
31. Jiang WJ, Zhou R, Li PJ, Sun YL, Lu QF, Qiu Y, et al. Protective effect of chrysophanol on LPS/D-GalN-induced hepatic injury through the RIP140/NF-kappa B pathway. *Rsc Adv* 2016;**6**:38192–200.
32. Feng Y, Huang SL, Dou W, Zhang S, Chen JH, Shen Y, et al. Emodin, a natural product, selectively inhibits 11β-hydroxysteroid dehydrogenase type 1 and ameliorates metabolic disorder in diet-induced obese mice. *Br J Pharmacol* 2010;**161**:113–26.
33. Monisha BA, Kumar N, Tiku AB. Emodin and its role in chronic diseases. *Adv Exp Med Biol* 2016;**928**:47–73.
34. Li N, Tian Y, Wang C, Zhang P, You S. Protective effect of Lai Fu Cheng Qi decoction on severe acute pancreatitis-induced myocardial injury in a rat model. *Exp Ther Med* 2015;**9**:1133–40.
35. Hosseini A, Rajabian A. Protective effect of *Rheum turkestanikum* root against doxorubicin-induced toxicity in H9c2 cells. *Rev Bras Farmacogn* 2016;**26**:347–51.
36. Hosseini A, Mollazadeh H, Amiri MS, Sadeghnia HR, Ghorbani A. Effects of a standardized extract of *Rheum turkestanicum* Janischew root on diabetic changes in the kidney, liver and heart of streptozotocin-induced diabetic rats. *Biomed Pharmacother* 2017;**86**:605–11.
37. Lu J, Zhang RW, Hong HQ, Yang ZL, Sun DP, Sun SY, et al. The poly(ADP-ribosyl)ation of FoxO3 mediated by PARP1 participates in isoproterenol-induced cardiac hypertrophy. *Biochim Biophys Acta* 2016;**1863**:3027–39.
38. Xu S, Bai P, Little PJ, Liu P. Poly(ADP-ribose) polymerase 1 (PARP1) in atherosclerosis: from molecular mechanisms to therapeutic implications. *Med Res Rev* 2014;**34**:644–75.
39. Magan N, Isaacs RJ, Stowell KM. Treatment with the PARP-inhibitor PJ34 causes enhanced doxorubicin-mediated cell death in HeLa cells. *Anticancer Drugs* 2012;**23**:627–37.
40. Mariano G, Ricciardi MR, Trisciuoglio D, Zampieri M, Ciccarone F, Guastafierro T, et al. PARP inhibitor ABT-888 affects response of MDA-MB-231 cells to doxorubicin treatment, targeting Snail expression. *Oncotarget* 2015;**6**:15008–21.
41. Lin YW, Kang TB, Zhou BHP. Doxorubicin enhances SNAIL/LSD1-mediated PTEN suppression in a PARP1-dependent manner. *Cell Cycle* 2014;**13**:1708–16.
42. Chowdhury P, Nagesh PKB, Khan S, Hafeez BB, Chauhan SC, Jaggi M, et al. Development of polyvinylpyrrolidone/paclitaxel self-assemblies for breast cancer. *Acta Pharm Sin B* 2018;**8**:602–14.
43. Mason KA, Valdecanas D, Hunter NR, Milas L. INO-1001, a novel inhibitor of poly(ADP-ribose) polymerase, enhances tumor response to doxorubicin. *Invest New Drugs* 2008;**26**:1–5.
44. Pacher P, Liaudet L, Bai P, Virag L, Mabley JG, Hasko G, et al. Activation of poly(ADP-ribose) polymerase contributes to development of doxorubicin-induced heart failure. *J Pharmacol Exp Ther* 2002;**300**:862–7.
45. Bartha E, Solti I, Szabo A, Olah G, Magyar K, Szabados E, et al. Regulation of kinase cascade activation and heat shock protein expression by poly(ADP-ribose) polymerase inhibition in doxorubicin-induced heart failure. *J Cardiovasc Pharmacol* 2011;**58**:380–91.
46. Efremova AS, Shram SI, Myasoedov NF. Doxorubicin causes transient activation of protein poly(ADP-ribosyl)ation in H9c2 cardiomyocytes. *Dokl Biochem Biophys* 2015;**464**:333–7.
47. Szenczi O, Kemecsei M, Holthuijsen MFJ, van Riel NAW, van der Vusse GJ, Pacher P, et al. Poly(ADP-ribose) polymerase regulates myocardial calcium handling in doxorubicin-induced heart failure. *Biochem Pharmacol* 2005;**69**:725–32.
48. Lin FL, Lin CH, Ho JD, Yen JL, Chang HM, Chiou GCY, et al. The natural retinoprotectant chrysophanol attenuated photoreceptor cell apoptosis in an *N*-methyl-*N*-nitrosourea-induced mouse model of retinal degenaration. *Sci Rep* 2017;**7**:41086.
49. Lu J, Sun DP, Liu ZP, Li M, Hong HQ, Liu C, et al. SIRT6 suppresses isoproterenol-induced cardiac hypertrophy through activation of autophagy. *Transl Res* 2016;**172**:96–112.
50. Lu J, Sun DP, Gao S, Gao Y, Ye JT, Liu PQ. Cyclovirobuxine D induces autophagy-associated cell death *via* the Akt/mTOR pathway in MCF-7 human breast cancer cells. *J Pharmacol Sci* 2014;**125**:74–82.
51. Chen JL, Ma MM, Lu YW, Wang LS, Wu CS, Duan HF. Rhaponticin from Rhubarb Rhizomes alleviates liver steatosis and improves blood glucose and lipid profiles in KK/Ay diabetic mice. *Planta Med* 2009;**75**:472–7.
52. Pillai JB, Gupta M, Rajamohan SB, Lang R, Raman J, Gupta MP. Poly (ADP-ribose) polymerase-1-deficient mice are protected from angiotensin II-induced cardiac hypertrophy. *Am J Physiol Heart Circ Physiol* 2006;**291**:H1545–53.
53. Paradis P, Dali-Youcef N, Paradis FW, Thibault G, Nemer M. Overexpression of angiotensin II type I receptor in cardiomyocytes induces cardiac hypertrophy and remodeling. *Proc Natl Acad Sci U S A* 2000;**97**:931–6.
54. De Flora A, Zocchi E, Guida L, Franco L, Bruzzone S. Autocrine and paracrine calcium signaling by the CD38/NAD^+/cyclic ADP-ribose system. *Ann N Y Acad Sci* 2004;**1028**:176–91.
55. Feng GS, Zhu CG, Li ZM, Wang PX, Huang Y, Liu M, et al. Synthesis of the novel PARP-1 inhibitor AG-690/11026014 and its protective effects on angiotensin II-induced mouse cardiac remodeling. *Acta Pharmacol Sin* 2017;**38**:638–50.
56. Feng XJ, Gao H, Gao S, Li ZM, Li H, Lu J, et al. The orphan receptor NOR1 participates in isoprenaline-induced cardiac hypertrophy by regulating PARP-1. *Br J Pharmacol* 2015;**172**:2852–63.
57. Liu M, Li Z, Chen GW, Li ZM, Wang LP, Ye JT, et al. AG-690/11026014, a novel PARP-1 inhibitor, protects cardiomyocytes from Ang II-induced hypertrophy. *Mol Cell Endocrinol* 2014;**392**:14–22.
58. Liu M, Ye JT, Gao S, Fang W, Li H, Geng BA, et al. Salvianolic acid B protects cardiomyocytes from angiotensin II-induced hypertrophy *via* inhibition of PARP-1. *Biochem Biophys Res Commun* 2014;**444**:346–53.